Dark Energy Perturbations

Comparing quintessence and tachyonic perturbations.

Manvendra Pratap Rajvanshi

IISER Mohali

TABLE OF CONTENTS

Accelerated Expansion

- Cosmological observations(Supernovae IA and other observations) suggest that the Universe's expansion rate is increasing.

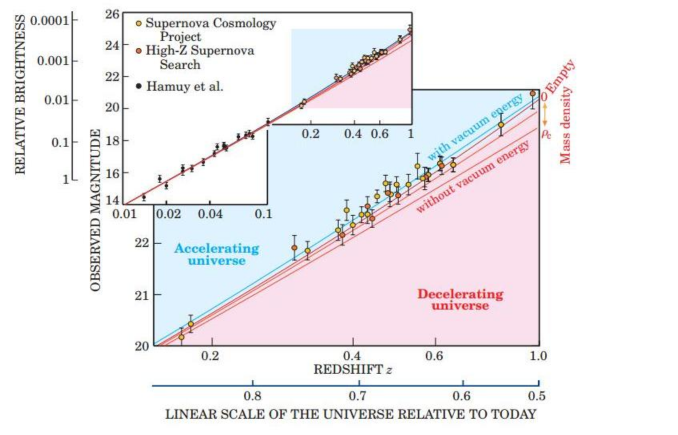

Figure: Observations from supernovae suggest that universe is in mode of accelerated expansion.[Image Source:Supernovae, Dark Energy, and the Accelerating Universe, Saul Perlmutter, PhysicsToday 2003]

Beyond Λ: A plethora of theories[1] proposed

Although, ΛCDM has been phenomenal in comparisons with data, theoretical basis of such a constant is problematic. There are issues like fine-tuning problem, coincidence problem, etc. This provides motivation for looking for models beyond Λ. Some that are relevant in context of this discussion:

- Quintessence
- Tachyonic
- Effective fluids
- K-essence
- Chaplygin gas

Cosmological Constant acts as dark energy with a constant density and pressure. In contrast, in other theories of dark energy e.g. quintessence, chaplygin gas, tachyonic field,k-essence, etc. density and pressure can vary in space-time.

[1] L. Amendola and S. Tsujikawa, Dark Energy: Theory and Observations. Cambridge University Press, 2010

Scalar Field Models

- Quintessence[2] is canonical scalar field minimally coupled to metric. Its Lagrangian is:

$$L_{quint} = \partial_\mu \phi \partial^\mu \phi - V(\phi)$$

- Lagrangian for Tachyonic fields[3] is field theory analogue of Lagrangian for relativistic particles:

$$L_{tach} = -V(\phi)\sqrt{1 - \partial_\mu \phi \partial^\mu \phi}$$

- More generally a scalar field Lagrangian can be written as:

$$L_{sf} = f(K, \phi)$$

where

$$K = \partial_\mu \phi \partial^\mu \phi$$

[2] S. Tsujikawa, Quintessence: A Review, Class. Quant. Grav. 30 (2013) 214003 [1304.1961].
[3] J. Bagla, H. K. Jassal and T. Padmanabhan, Cosmology with tachyon field as dark energy, Phys. Rev. D 67 (2003) 063504 [astro-ph/0212198].

Different Levels of Cosmological Calculations

- Background Cosmology: Based on assumption of homogeneity and isotropy.

$$ds^2 = dt^2 - a^2(dx^2 + dy^2 + dz^2)$$

$$\frac{\ddot{a}}{a} = -\frac{4\pi G}{3}[\rho(1 + 3w)]$$

- Linear Perturbations: First order approximations to background metric/dynamics:

$$ds^2 = (1 + A)dt^2 - B_i dt dx^i - a^2(\delta_{ij} + \eta_{ij})dx^i dx^j$$

- Nonlinear Simulations in some symmetries/special cases: spherical, ellipsoidal collapse, etc.
- N-body simulations: many diverse approximations/implementations.

Questions that we look into:

- Methods need to be developed that can help distinguish between these models. Study of perturbations can help achieve this as perturbations might evolve differently in different models. Perturbations are studied at varying level of approximations. This sets the context for this thesis. In this thesis, we study nonlinear(as well as linear) perturbations in scalar field based dark energy models: quintessence and tachyonic fields.
- Probing the effects coming from nonlinear relativistic simulations in spherical symmetry. Here we start from action and derive equations with no approximations about clustering of DE but spherical symmetry.
- We ask if two scalar field dark energy models(Lagrangians) which give exactly same results for evolution of background, can be distinguished by perturbations: linear and nonlinear level.
- If ignoring spatial fluctuations in an effective description will have any observable effect.
- Study the evolution of spacetime fluctuations in dark energy field.

Outline of this project

- Nonlinear spherically symmetric perturbations in quintessence dark energy cosmology.
- Reconstruction of quintessence and tachyonic potentials for given background expansion.
- Non-linear spherical collapse in tachyon models and a comparison of collapse in tachyon and quintessence models of dark energy
- Comparison on perturbations in cosmological linear perturbation theory and efficiency of linear perturbations to distinguish two models under CMB data.

Spherically Symmetric Perturbations

Spherical Collapse visual

Spherically Symmetric Perturbations: Metric

For modelling spatially isotropic perturbations, we start by considering a general spatially isotropic metric:

$$ds^2 = -e^{(2B)}dr^2 - R^2(d\theta^2 + sin^2\theta d\phi^2) + dt^2 \quad (1)$$

where $B(t, r)$ and $R(t, r)$ are arbitrary functions of r and t.

Equations for Quintessence

$$
\begin{aligned}
\ddot{B} &= -c^2 e^{-2B}\frac{R'^2}{R^2} + \frac{c^2}{R^2} + \frac{\dot{R}^2}{R^2} - \dot{B}^2 - 4\pi G\rho - \frac{8\pi G}{c}\left[\frac{\dot{\Phi}^2}{2c^2} - e^{-2B}\frac{\Phi'^2}{2}\right] \\
\frac{\ddot{R}}{R} &= -\frac{4\pi G}{c}\left[\frac{\dot{\Phi}^2}{2c^2} + \frac{e^{-2B}\Phi'^2}{2} - V\right] - \frac{1}{2}\frac{\dot{R}^2}{R^2} + \frac{c^2}{2}\left[e^{-2B}\frac{R'^2}{R^2} - \frac{1}{R^2}\right] \\
\ddot{\Phi} &= c^2\left[-\frac{\partial V}{\partial \Phi} + e^{-2B}\left\{\Phi'' - \left(B' - \frac{2R'}{R}\right)\Phi'\right\}\right] - \left(\dot{B} + \frac{2\dot{R}}{R}\right)\dot{\Phi}
\end{aligned}
$$

Here a dash represents a partial derivative with respect to *r* and a dot represents a partial derivative with respect to *t*.

Virialization

The solutions of system of equations, for spherical collapse, lead to a singularity. Each shell reaches turn around and collapses to origin. This is the "mathematical solution". In real world, perturbations collapse to form stable/pseudo-stable structures, they "virialise"[4]. a simplistic approach assuming that in-falling perturbation stabilizes at radius where kinetic energy and potential energy satisfy virial theorem:

$$< T > + \frac{1}{2} \langle R F_R \rangle = 0 \quad (2)$$

here T is the kinetic energy, R is the radius of the shell and F_R is the radial force on the shell.

[4] I. Maor and O. Lahav, On virialization with dark energy, Journal of Cosmology and Astroparticle Physics 2005 (2005) 003

Turn around and Virial Characteristics

Properties of spherical perturbations at turn around and virialization are dependent on cosmology. For example:

- In case of Einstein-deSitter universe, the radius of the virialised halo is exactly half of the maximum or the turn around radius for the shell.
- In case of ΛCDM,

$$R_V = \left(\frac{2}{3}\right)^{1/3} \left(\frac{\Omega_\Lambda R_T^3 + \Omega_M (\frac{a_0}{a_{in}})^3 (1+\delta_{in}) R_{in}^3}{\Omega_\Lambda R_T}\right)^{1/2}$$

$$\sin\left[\frac{1}{3}\arcsin\left\{\frac{\Omega_M a_0^3 (1+\delta_{in}) R_{in}^3}{a_{in}^3 R_T^3}\left(\frac{1.5}{1+\frac{\Omega_M}{\Omega_\Lambda}(\frac{a_0 R_{in}}{a_{in} R_T})^3 (1+\delta_{in})}\right)^{3/2}\right\}\right]$$

RESULTS for QUINTESSENCE

Effects on Dark Matter Perturbations

- For studying the effects of dark energy perturbations on dark matter clustering, we run besides quintessence simulations, corresponding simulations with a non-clustering fluid with same equation of state as that in quintessence case. We call it $w(z)$ fluid.
- We show results for both- overdense and underdense spherical halos. While overdense results involve virialisation, underdense cases do not have assumptions related to virialisation.

Effects on matter clustering

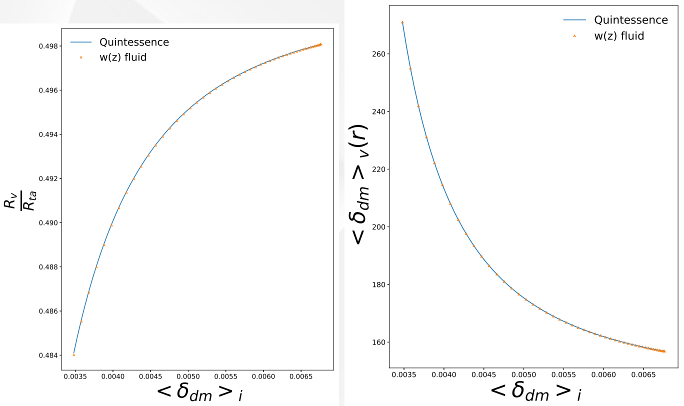

Figure: Markers(w(z) fluid) represent a non-clustering fluid implementation which has same background evolution. These show that the induced DE fluctuations, shown in coming figures, do not have significant effect on matter.

Overdense Case: Perturbations in DE

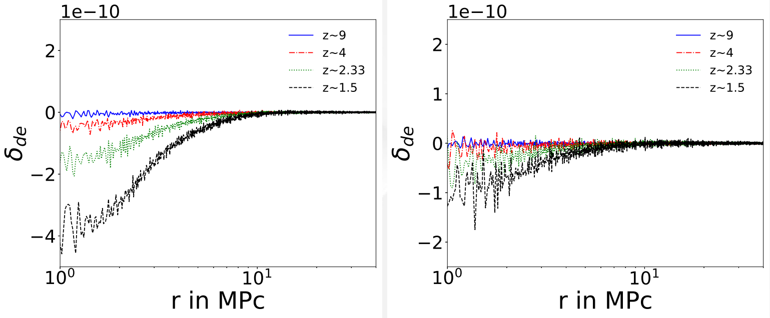

Figure: Density contrast for dark energy as a function of scale at different epochs. We see that the amplitude of perturbations in dark energy remains small at all scales and at all times. The left panel is for $V \propto \psi^2$ while the right panel is for $V \propto \exp(-\psi)$.

Spatio-temporal Fluctuations in Dark Energy

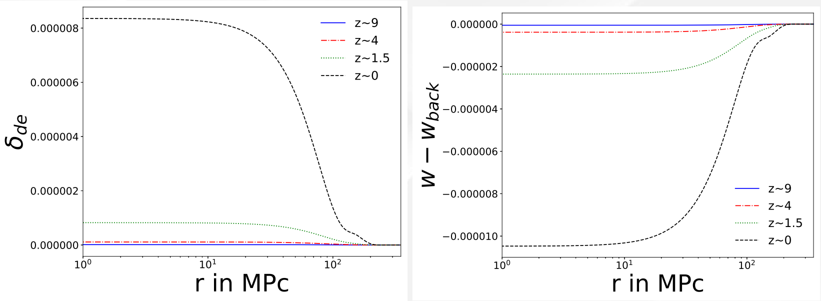

Figure: Fluctuations develop in dark energy field, which was set homogeneous at initial time at $z \sim 1000$. This is an initially underdense halo (void).

Spatio-temporal Fluctuations in Dark Energy

Spatio-temporal Fluctuations in Dark Energy visual

Comparison with linear theory

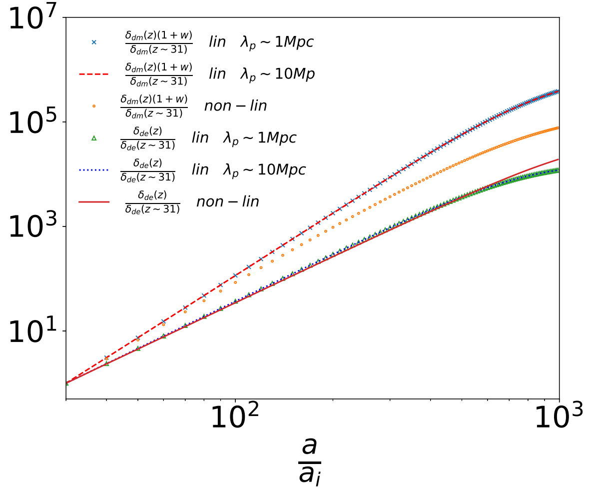

Figure: A comparison of the evolution of dark energy perturbations.
At very large scales the linear theory prediction for the magnitude of dark energy perturbations scales as $(1+w)\delta_{dm}$. The linear evolution for dark energy perturbations is slower at small scales as compared to the expected variation at large scales.

Significance of spatial gradients

$$\ddot{\Phi} = c^2 \left[-\frac{\partial V}{\partial \Phi} + e^{-2B} \left\{ \Phi'' - \left(B' - \frac{2R'}{R} \right) \Phi' \right\} \right] - \left(\dot{B} + \frac{2\dot{R}}{R} \right) \dot{\Phi}$$

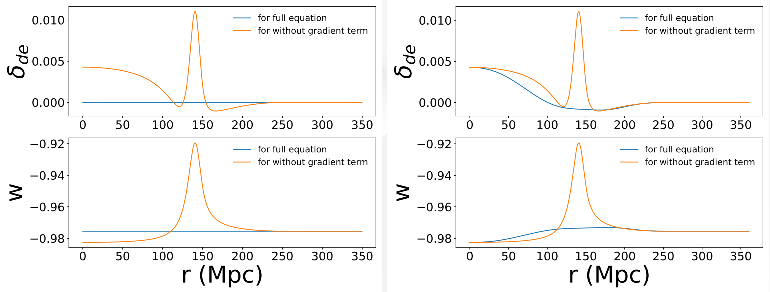

Figure: We show the variation computed by retaining only the local Hubble expansion terms in the equation of motion and compare it with the full simulation. In the former case, we ignore the gradient term. We find that the variation of w is fairly strong and has some localised features when the gradient terms are ignored. The localised features are not present in the full simulation indicating that the gradients of the scalar field are suppressed in the evolution, and the local Hubble expansion is not the only determining factor.

Reconstruction of Potentials

Need for reconstruction

- Give a particular potential(with its parameters) for a scalar field, it gives a particular evolution.
- In context of cosmology, a particular potential leads a specific $w(z)$ and a specific expansion history.
- For the purpose of studying the differences in perturbations in different scalar field models, we need to understand which effects are due to differences in expansion history and which are due to differences in dynamics of perturbations.
- Since, background expansion is already constrained, by data, to be close to $\Lambda(w \sim -1)$. Theories often have tunable parameters which are then constrained to bring the expansion close to Λ.

Reconstruction

Given a particular $w(z)$, we want to find the corresponding potentials for quintessence and tachyonic models, that simulate the prescribed $w(z)$.
We focus on two particular form of $w(z)$ or $w(a)$:

- Constant w: $w(a) = constant$
- Chevallier-Polarski-Linder(CPL) paramterization[5,6]

$$w = w_0 + w_a(1 - \frac{a}{a_0})$$

But we develop and use a numerical scheme for any $w(a)$.

[5] M. Chevallier and D. Polarski, Accelerating Universes with Scaling Dark Matter, International Journal of Modern Physics D 10 (2001) 213

[6] E. V. Linder, Exploring the Expansion History of the Universe, Phys. Rev. Lett. 90 (2003) 091301

Reconstruction of Potentials

For an arbitrary function $w(a)$, continuity equation for that component gives:

$$\rho_\phi = \rho_{\phi_i} \exp\left[-3\int \frac{1+w}{a} da\right]$$

Equivalently

$$\Omega_\phi := \frac{8\pi G \rho_\phi}{3H_i^2} = \Omega_{\phi_i} e^{-3\int \frac{1+w}{a} da}$$

$$\frac{d\phi_{tach}}{da} = \frac{\sqrt{1+w}}{\sqrt{\frac{\alpha}{a} + a^2 \Omega_{\phi tach}}}$$

$$\frac{d\phi_q}{da} = \frac{\sqrt{3(1+w)\Omega_{\phi q}}}{\sqrt{8\pi G}\sqrt{\frac{\alpha}{a} + a^2 \Omega_{\phi q}}}$$

$$\frac{V(a)}{H_i^2} = \frac{3(1-w)\Omega_{\phi q}}{16\pi G}$$

$$\frac{V(a)}{H_i^2} = \frac{3\sqrt{-w}\,\Omega_{\phi tach}}{8\pi G}$$

Reconstruction: Numerical Approach

One can numerically integrate equations to get $\phi(a)$ and $V(a)$. Hence one can obtain a numerical table of $V(\phi)$ vs ϕ in desired range.
This table can be used for numerical fitting or interpolation functions.
For example, cubic splines can be used for fitting to obtain spline coefficients which can be used for calculating $V(\phi)$ and its gradients given a value of ϕ.
Once we have spline coefficients and ϕ, task is to find the interval in which the value of ϕ lies so that we can use coefficients corresponding to that interval.

Tachyon field:Constant w scenario

The integral for tachyonic field takes following form for constant w:

$$\phi(a) = \int \frac{\sqrt{a(1+w)}}{\sqrt{\alpha + \frac{\beta}{a^{3w}}}} da \tag{3}$$

Defining:

$$x^2 = \alpha + \frac{\beta}{a^{3w}} \tag{4}$$

reduces the integral to form:

$$\phi(x) = \int \frac{\sigma}{(x^2 - \alpha)^k} dx \tag{5}$$

where σ and k are:

$$\sigma = \frac{2\sqrt{1+w}}{3w\beta} \beta^{\frac{w+\frac{1}{2}}{w}} \qquad k = \frac{w+\frac{1}{2}}{w} \tag{6}$$

Tachyon field: Constant w scenario...

Integral in eq.(5) is trivial for $w = -\frac{1}{2}$ where we get:

$$\phi(a) = \sqrt{\frac{\sigma}{\alpha + \beta a^{3/2}}} \tag{7}$$

Potential $V(a)$ for constant w case is:

$$\frac{V(a)}{H_i^2} = \frac{3\sqrt{-w}\beta}{8\pi G a^{3(1+w)}} \tag{8}$$

When $w = -\frac{1}{2}$, we get:

$$\frac{V(a)}{H_i^2} = \frac{3\beta}{8\pi G\sqrt{2}\left[\frac{\sigma}{\phi^2\beta} - \frac{\alpha}{\beta}\right]} \tag{9}$$

Tachyon field:Constant w scenario...

For other values of *w*, integral in equation (3) does not give a closed formula. We use MATHEMATICA to do this integral and get result in form of Hypergeometric2F1 functions:

$$\phi(a) = \frac{2a\sqrt{a(w+1)}\sqrt{\frac{\beta a^{-3w}+\alpha}{\alpha}}\,{}_2F_1\left[\frac{1}{2}, -\frac{1}{2w}; 1-\frac{1}{2w}; -\frac{a^{-3w}\beta}{\alpha}\right]}{3\sqrt{\beta a^{-3w}+\alpha}} \tag{10}$$

Equation (3) can be written in the form of a differential equation. Let

$$z = -\frac{a^{-3w}\beta}{\alpha} \tag{11}$$

Then eq.(3) can be differentiated to obtain:

$$z(1-z)\frac{d^2\phi}{dz^2} + \left[\left(\frac{1}{2w}+1\right) - \left(\frac{3}{2}+\frac{1}{2w}\right)z\right]\frac{d\phi}{dz} = 0 \tag{12}$$

It can be integrated twice to obtain $\phi(z)$ in terms of incomplete beta functions($B(z;a,b)$), which can be related to ${}_2F_1(a,b,c,z)$:

$$\phi(z) = C_1 B(z;1-u,1+u+v) + C_2 \tag{13}$$

$$\begin{aligned} u &= \left(\frac{1}{2w}+1\right) \\ v &= -\left(\frac{3}{2}+\frac{1}{2w}\right) \end{aligned} \tag{14}$$

$B(z;a,b)$ is related to ${}_2F_1(a,b,c,z)$:

$$B(z;a,b) = \frac{z^a}{a}\,{}_2F_1(a,1-b,a+1,z) \tag{15}$$

Quintessence field: Constant w scenario

For $w(a) = constant$ case, one can obtain a closed formula for $V(\phi)$. In this case,:

$$\frac{d\phi}{dt} = \sqrt{(1+w)\frac{3}{8\pi G}\frac{\beta}{a^{3(1+w)}}} \tag{16}$$

and

$$\frac{d\phi}{da} = \sqrt{\frac{3(1+w)}{8\pi G}}\sqrt{\left[\frac{1}{\frac{\alpha a^{3w}}{\beta}+1}\right]}\left(\frac{1}{a}\right) \tag{17}$$

Defining:

$$\lambda = \sqrt{\frac{3(1+w)}{8\pi G}} \tag{18}$$

and

$$x^2 = \frac{\alpha a^{3w}}{\beta} + 1 \tag{19}$$

Then

$$\phi(x) = C_1 + \frac{2\lambda}{3w}\int \frac{dx}{x^2-1} \tag{20}$$

Quintessence field: Constant w scenario

Solution is :

$$\phi(x) = -\frac{\lambda}{3w}[log(1+x) - log(x-1)] \tag{21}$$

Inverting this we get:

$$x = \frac{e^{-3w\phi/\lambda} + 1}{e^{-3w\phi/\lambda} - 1} \tag{22}$$

Defining:

$$m = -\frac{3w\phi}{2\lambda} \tag{23}$$

We rewrite eq.(22):

$$x = \coth m \tag{24}$$

We get

$$a^{3w} = \frac{\beta}{\alpha}\left[(\coth m)^2 - 1\right] \tag{25}$$

$$\frac{V(\phi)}{H_i^2} = \frac{3(1-w)\beta}{16\pi G}\left[\frac{\alpha}{\beta}\sinh^2\left(-\frac{3w\phi\sqrt{8\pi G}}{2\sqrt{3(1+w)}}\right)\right]^{\frac{(1+w)}{w}} \tag{26}$$

Spherical collpase in tachyonic models and comparsion with quintessence

Equations for Tachyonic DE

$$
\begin{aligned}
\ddot{B} &= -c^2 e^{-2B}\frac{R'^2}{R^2} + \frac{c^2}{R^2} + \frac{\dot{R}^2}{R^2} - \dot{B}^2 - 4\pi G\rho + \frac{4\pi G V}{c^2}\left[\frac{e^{-2B}\Phi'^2 - \dot{\Phi}^2}{\sqrt{1-u^2}}\right] \\
\frac{\ddot{R}}{R} &= \frac{4\pi G V}{c\sqrt{1-u^2}}\left[1 - u^2 - e^{-2B}\Phi'^2\right] - \frac{1}{2}\frac{\dot{R}^2}{R^2} + \frac{c^2}{2}\left[e^{-2B}\frac{R'^2}{R^2} - \frac{1}{R^2}\right]
\end{aligned}
$$

$$
\begin{aligned}
\ddot{\Phi}RV(e^{2B} + \Phi'^2) &= 2e^{2B}VR'\Phi'^3 - 2V\dot{R}\dot{\Phi}\Phi'^2 + 2VR'\Phi''(1-\dot{\Phi}^2) - RV_{,\Phi}\Phi'^2 \\
&\quad - RVB'\Phi'(1-\dot{\Phi}^2) + RV\Phi''(1-\dot{\Phi}^2) - 2RV\dot{\Phi}\dot{B}\Phi'^2 \\
&\quad + 2RV\dot{\Phi}\Phi'\dot{\Phi}' \\
&\quad - RV_{,\Phi}e^{2B}(1-\dot{\Phi}^2) - V\dot{\Phi}(1-\dot{\Phi}^2)(R\dot{B} + 2\dot{R})e^{2B}
\end{aligned}
$$

Numerical Methods

- Set up a grid in r and evolve all quantities on this grid using RK4 scheme. At each time step(sub-step), we calculate gradients using 3/5 order finite difference schemes.
- **For use of reconstructed potential:** Cubic splines can be used for fitting to obtain spline coefficients which can be used for calculating $V(\phi)$ and its gradients given a value of ϕ. Using the fact the at at outer radii, perturbations merge into background, we can start search for cubic interval from outside to inside. In this way for each new inner point one has to only search in the adjacent intervals for interpolation if the field is continuous.

Perturbations in Tachyonic DE

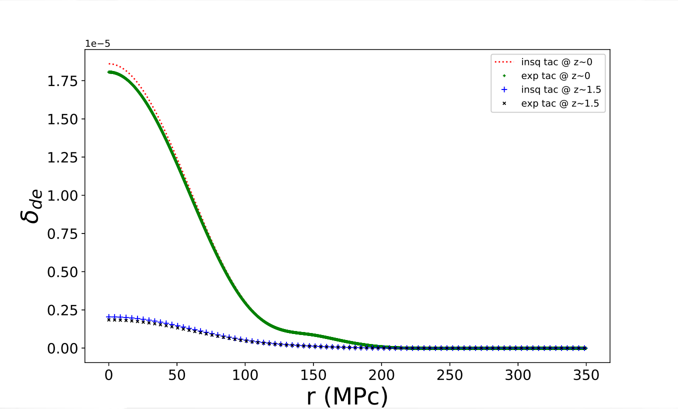

Figure: Dark energy(DE) density contrast as a function of comoving radius at two different redshifts. Here the initial matter perturbation was underdense. There was no perturbation in DE at initial time, but metric perturbations induce perturbation in DE field. This perturbation grows stronger with time as can be seen from curves at 2 different redshifts.

Comparing perturbations: Quintessence vs Tachyonic

- We do spherical collapse simulations with reconstructed potentials, so the background expansion is same for both quintessence and tachyonic fields.
- For the purpose of comparisons, we expansion corresponding to following forms of $w(z)$:
  - Constant w: $w(a) = constant$
  - Chevallier-Polarski-Linder(CPL) paramterization

$$w = w_0 + w_a(1 - \frac{a}{a_0})$$

  we have $w_0 = -0.9$ and $w_a = \pm 0.09$. In figures we represent cases with $w_a = +0.09$ with notation "cpl+" and $w_a = -0.09$ model with "cpl-".

Tachyonic vs Quintessence: Matter Perturbations

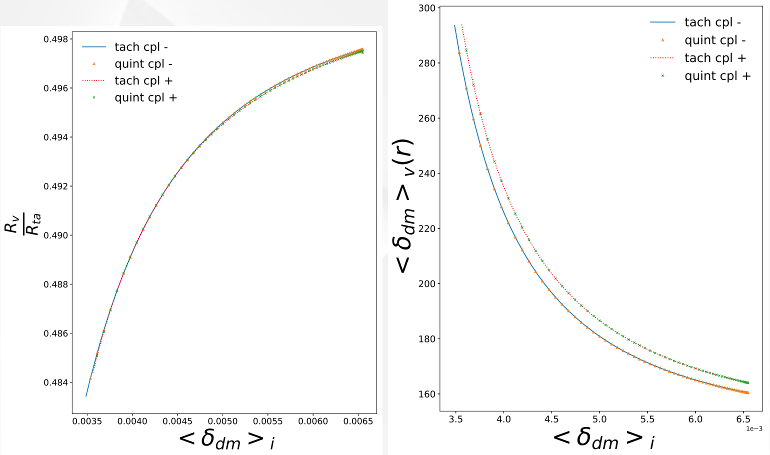

Figure: Virial characteristics for CPL case. Left panel shows ratio of virial radius to turn around radius as a function of the initial density contrast in dark matter. Right panel shows Density contrast at virialisation as a function of the initial density contrast in dark matter. "quint" denotes quintessence and "tach" represents tachyonic field. cpl+ denotes $w_a = +0.09$ and cpl- represents $w_a = -0.09$.

Tachyonic vs Quintessence: Matter Perturbations

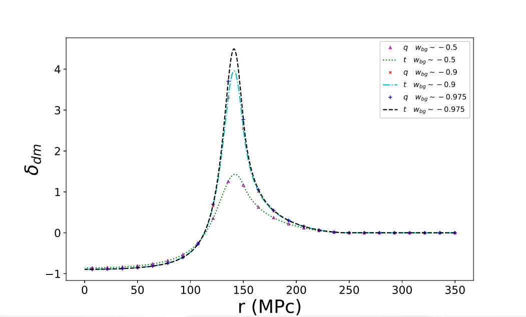

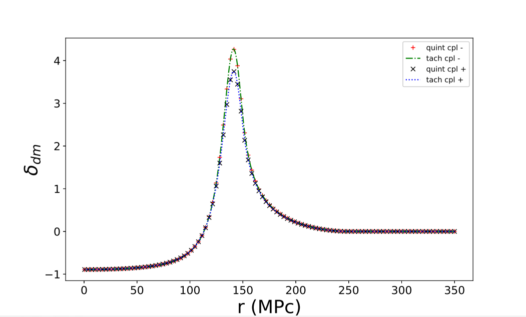

Figure: Top panel shows comparisons for different constant w backgrounds, while bottom panel shows the cases for two CPL models.

Tach vs Quintessence: Dark Energy Perturbations

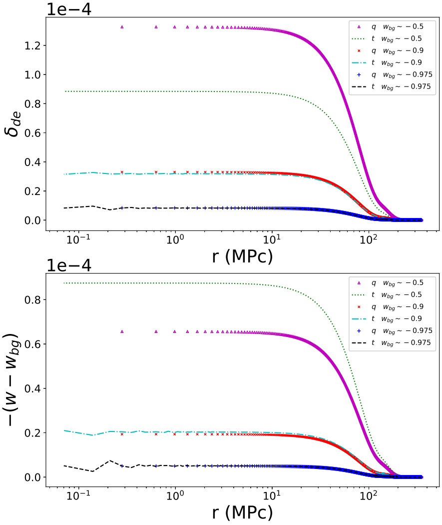

Tachyon-Quintessence comparisons: Summary

- We find that evolution of dark matter perturbations depends only on the expansion history. There is no discernable imprint of the dark energy model on the evolution of dark matter perturbations.
- The amplitude of dark energy perturbations depends on the expansion history as well as the dark energy model (tachyon/quintessence). *Thus in principle there is an observable signature of the class of dark energy models, though the differences are very small*.
- These differences are larger for models that deviate significantly from the ΛCDM model in terms of the expansion history.
- We may choose any dark energy model to reproduce the appropriate expansion history as the evolution of dark matter perturbations is insensitive to the specifics of the dark energy model other than the expansion history.

Quintessence and Tachyonic visual

Tachyonic vs Quintessence dark energy: prospects of distinguishing them using linear perturbations and CMB data

Linear Perturbations

Linear theory calculations do not assume any symmetry, but are valid for small perturbations only. Linear Theory of Cosmological Perturbations[7] forms the basis for most of the calculations in modern (beyond FLRW) cosmology.

If $\bar{g}_{\mu\nu}$ is background metric and $g_{\mu\nu}$ is the metric with perturbations $\delta g_{\mu\nu}$, then

$$g_{\mu\nu} \approx \bar{g}_{\mu\nu} + \delta g_{\mu\nu} \tag{27}$$

Here we only consider scalar metric perturbations:

$$ds^2 = (1 + 2\psi)dt^2 - (1 - 2\xi)a^2(dx^2 + dy^2 + dz^2) \tag{28}$$

[7] H. Kodama and M. Sasaki, Cosmological Perturbation Theory, Prog. Theor. Phys. Suppl. 78 (1984) 1.

Linear Equations

$$6\frac{\psi}{a^2}\left[\frac{a'^2}{a^2}-2\frac{a''}{a}\right]-12\frac{a'}{a}\frac{\phi'}{a^2}-6\frac{a'}{a}\frac{\psi'}{a^2}-6\frac{\phi''}{a^2}+2\frac{\Delta}{a^2}[\phi-\psi] \\ =8\pi G(\delta T_1^1+\delta T_2^2+\delta T_3^3) \tag{29}$$

$$\sum_{i=1}^{3}\left[\frac{a'}{a}\frac{\partial\psi}{\partial x^i}+\frac{\partial\phi'}{\partial x^i}\right]=4\pi Ga^2\sum_{i=1}^{3}\delta T_i^0 \tag{30}$$

$$\left[\frac{\partial^2}{\partial x^1\partial x^2}+\frac{\partial^2}{\partial x^2\partial x^3}+\frac{\partial^2}{\partial x^3\partial x^1}\right](\psi-\phi)=8\pi Ga^2(\delta T_2^1+\delta T_3^2+\delta T_1^3) \tag{31}$$

$$-3\frac{a'^2}{a^2}\psi-3\frac{a'}{a}\phi'+\Delta\phi=4\pi Ga^2\delta T_0^0 \tag{32}$$

Here δT represent first order perturbations to stress energy tensor and Δ is Laplacian operator defined as:

$$\Delta\equiv\sum_{i=1}^{3}\frac{\partial^2}{\partial x^{i2}} \tag{33}$$

Linear Equations

. Decomposing pressure and density in background+perturbation:

$$\rho(x,y,z,t) = \bar{\rho}(t)(1+\delta_m(x,y,z,t)) \quad (34)$$

$$p = \bar{p} + \delta p \quad (35)$$

and we have velocity perturbations(background/average velocity is 0) defined as:

$$v^i \equiv \frac{dx^i}{d\eta} \quad (36)$$

Then stress energy tensor for matter fluid is:

$$(\delta T^1_1 + \delta T^2_2 + \delta T^3_3) = -3\bar{\rho}c_s^2\delta_m \quad (37)$$

$$(\delta T^1_2 + \delta T^2_3 + \delta T^3_1) = 0 \quad (38)$$

$$\sum_{i=1}^{3} \delta T^0_i = \bar{\rho}\sum_{i=1}^{3} v_i \quad (39)$$

Defining Θ:

$$\Theta = \sum_{i=1}^{3} \frac{\partial v^i}{\partial x^i} = ik^j v_j \quad (40)$$

Continuity Equations

To obtain the equations of motion for density and velocity, we can use continuity equations:

$$T^{\mu}_{\nu\,;\mu} = 0 \tag{41}$$

We get

$$\delta'_m = -3\frac{a'}{a}(c_s^2 - w)\delta_m + 3(1+w)\phi' - (1+w)\Theta \tag{42}$$

$$\Theta' = -\left[\frac{a'}{a}(1-3w) + \frac{w'}{1+w}\right]\Theta + k^2\left[\frac{c_s^2\delta_m}{1+w} + \psi\right] \tag{43}$$

Scalar Fields and Effective Fluid Description

Let Φ be the field for a scalar field representing dark energy. Then its $T_{\mu\nu}$ can be written as:

$$T_{\mu\nu} = (\rho + P)v_\mu v_\nu - Pg_{\mu\nu} \tag{44}$$

where

$$v_\nu = \frac{\partial_\nu \Phi}{\sqrt{\partial^\alpha \Phi \partial_\alpha \Phi}} \tag{45}$$

Now we define first order quantities; density contrast and the corresponding quantity for EoS variation:

$$\rho = \bar{\rho}(1 + \delta) \qquad W = \bar{w}(1 + u) \tag{46}$$

where quantities with bar are background quantities dependent on time only. We also define:

$$\omega = 1 + \bar{w} \tag{47}$$

Effective pressure(P) for a scalar field theory is just the Lagrangian(L_Φ) of field while the effective density ρ is:

$$\rho = 2g^{\mu\nu} \frac{\partial L_\Phi}{\partial g^{\mu\nu}} - L_\Phi \tag{48}$$

Writing field as background+perturbation:

$$\Phi = \phi + (\delta\phi) \tag{49}$$

Writing scalar field eqs into fluid form

$$\dot{\delta} = 3u\frac{\dot{a}}{a}(1-\omega) + 3\dot{\psi}\omega + \frac{1}{4\pi G\bar{\rho}a^2}\nabla^2\left[\frac{\dot{a}}{a}\psi + \dot{\psi}\right] + \frac{\bar{\rho}_{dm}}{\bar{\rho}}\nabla^2 U \tag{50}$$

We also get a constrain equation for u

$$(-1+\omega)\frac{\partial u}{\partial x^j} = (1-\omega)\frac{\partial \delta}{\partial x^j} + \frac{\omega}{\dot{\phi}}\frac{\partial(\delta\phi)}{\partial x^j}\left[3\frac{\dot{a}}{a} + \frac{\dot{\bar{\rho}}}{\bar{\rho}} + \frac{\dot{\omega}}{\omega}\right] + \frac{\omega}{\dot{\phi}}\left[-\frac{\ddot{\phi}}{\dot{\phi}}\frac{\partial(\delta\phi)}{\partial x^j} + \frac{\partial(\delta\dot{\phi})}{\partial x^j}\right] - \omega\frac{\partial\psi}{\partial x^j} \tag{51}$$

$$\ddot{\psi} + 4\frac{\dot{a}}{a}\dot{\psi} + \psi\left[\frac{2\ddot{a}}{a} + \frac{\dot{a}^2}{a^2}\right] = -4\pi G\bar{\rho}(u+\delta)(1-\omega) \tag{52}$$

We observe that equations 50 and 52, explicitly do not have dependence on particular details of scalar field(if it is quintessence or tachyonic), but equation 51 does have such dependence. We rewrite this equations in less "field specific" forms and find that the equations in one of the field theory has more terms.

Rewriting equation into less field specific form

For tachyonic field equation 51 becomes:

$$\frac{(-1+\omega)}{2}\frac{\partial u}{\partial x^j} = (1-\omega)\frac{\partial\delta}{\partial x^j} + \left[3(1-\omega)\frac{\dot{a}}{a} + \frac{\dot{\omega}}{2\omega}\right] \left[\frac{1}{4\pi G\bar{\rho}}\left(\frac{\dot{a}}{a}\frac{\partial\psi}{\partial x^j} + \frac{\partial\dot{\psi}}{\partial x^j}\right) + a^2\frac{\bar{\rho}_{dm}}{\bar{\rho}}\frac{\partial U}{\partial x^j}\right] \quad (53)$$

While quintessence has some extra terms in addition to those present in equation 53:

$$\frac{(-1+\omega)}{2}\frac{\partial u}{\partial x^j} = (1-\omega)\frac{\partial\delta}{\partial x^j} + \left[3(1-\omega)\frac{\dot{a}}{a} + \frac{\dot{\omega}}{2\omega}\right] \left[\frac{1}{4\pi G\bar{\rho}}\left(\frac{\dot{a}}{a}\frac{\partial\psi}{\partial x^j} + \frac{\partial\dot{\psi}}{\partial x^j}\right) + a^2\frac{\bar{\rho}_{dm}}{\bar{\rho}}\frac{\partial U}{\partial x^j}\right] + \omega\left[\frac{3\dot{a}}{8\pi G\bar{\rho}a}\frac{\partial}{\partial x^j}\left(\frac{\dot{a}}{a}\psi + \dot{\psi}\right) + \frac{3\bar{\rho}_{dm}\dot{a}a}{2\bar{\rho}}\frac{\partial U}{\partial x^j} + \frac{1}{2}\frac{\partial\delta}{\partial x^j}\right] \quad (54)$$

Effects on Observables: w=-0.5

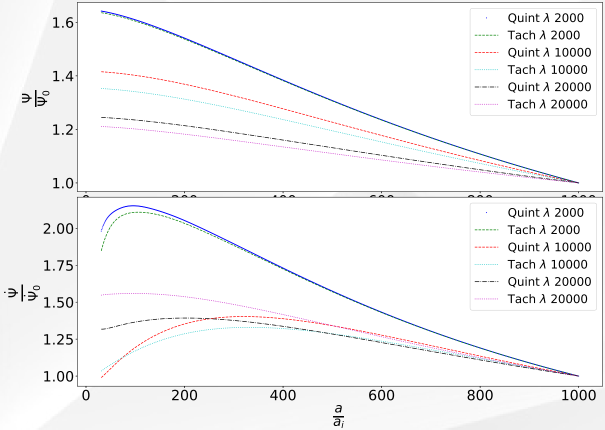

Figure: Potential ψ and its time derivatives for $\bar{w} = -0.5$ case. Potentials are normalized by their present day value(sub-scripted 0). Difference appears to be higher for $\lambda \sim 10k$.

Effects on Observables: w=-0.975

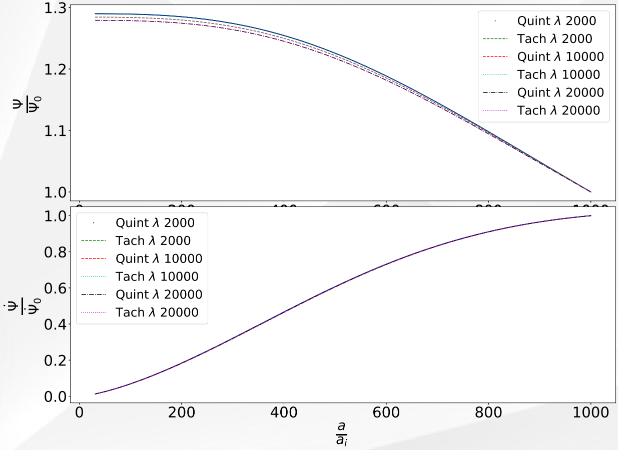

Figure: Potential ψ and its time derivatives for $\bar{w} = -0.975$ case. Clearly relative differences are much smaller than that in case of $w = -0.5$.

Describing scalar field using effective c_s^2

For scalar fields[8] , lets $L(X,\phi)$ be lagrangian density, where $X = \frac{1}{2}\partial_\mu\phi\partial^\mu\phi$ is kinetic term while ϕ is field. Rest frame for field is defined as one in which $(\delta\phi)$ vanishes. In arbitrary frame:

$$(\delta p) = \frac{\partial p}{\partial X}(\delta X) + \frac{\partial p}{\partial \phi}(\delta\phi) \tag{55}$$

with similar equation for $(\delta\rho)$. In rest frame:

$$(\delta p) = \frac{\partial p}{\partial X}(\delta X) \tag{56}$$

Combining equations for (δp) and $(\delta\rho)$ in rest frame:

$$c_s^2 = \frac{(\delta p)}{(\delta\rho)} = \frac{p_{,X}}{\rho_{,X}} \tag{57}$$

where $p_{,X}$ is partial derivative wrt X.

[8] Erickson et. al. Phys. Rev. Lett., vol. 88, p. 121301, 2002.

c_s^2 for tachyonic field

c_s^2 for quintessence is exactly one.
For tachyonic field lagrangian density is:

$$L(X, \Phi) = -V(\Phi)\sqrt{1 - 2X} \tag{58}$$

In rest frame of a scalar field:

$$c_s^2 = \frac{p_{,X}}{\rho_{,X}} = \frac{L_{,X}}{L_{,X} + 2L_{,XX}X} \tag{59}$$

In case of tachyonic field:

$$c_s^2 = (1 - 2X) = -\bar{w} - (1 + \bar{w})(\delta g^{00})_{rf} \tag{60}$$

In linear theory approximation, while using 60, one can ignore first order approximation and c_s^2 is just $-\bar{w}$.

Parametric form for c_s^2

We adopt following parametric form for c_s^2:

$$c_s^2 = c1 * w + c0 \tag{61}$$

This is a simplest form that can capture both quintessence and tachyonic models. For quintessence, we have $c1 = 0$ and $c0 = 1$ and for tachyonic models $c1 = -1$ and $c0 = 0$. We then do a MCMC sampling using CLASS with MontePython. We use CMB (Planck 2018 high-l TT,TE,EE, low-l EE, low-l TT, lensing) and BAO data(Boss Data Release 12, small-z BAO data from 6dF Galaxy Survey and SDSS DR7 main Galaxy sample). We find that the two parameters $c1$ and $c0$ remain unconstrained.

Data Constraints

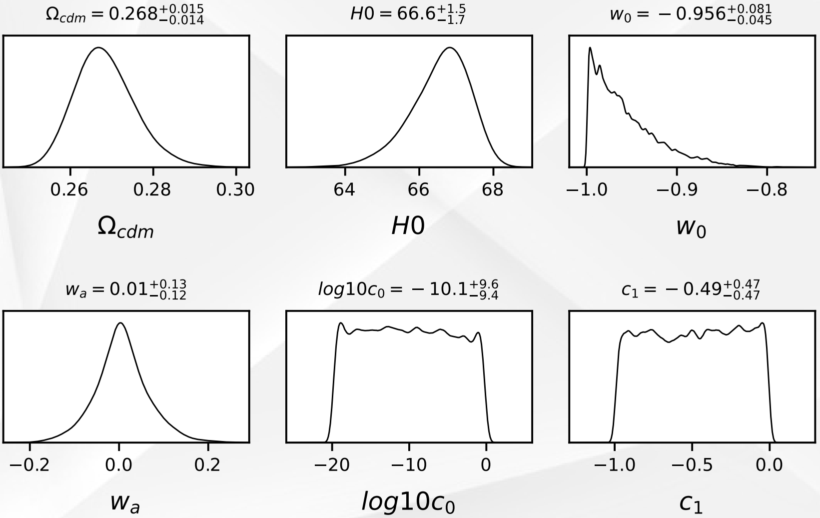

Figure: 1-dimensional posterior distributions.

Data Constraints

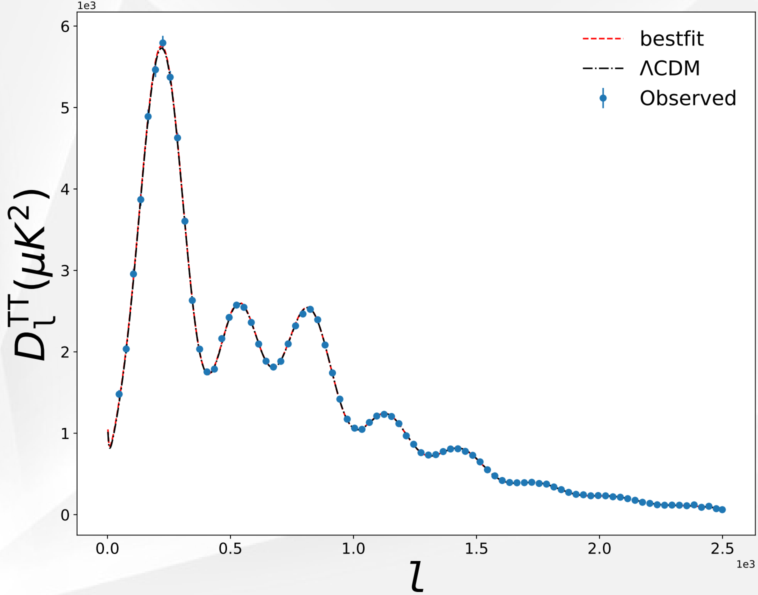

Constraining Tachyon Models using Data

We also modify the CLASS to implement tachyonic models as genuine scalar field at linear level, where equations are obtained from lagrangian corresponding to tachyonic dark energy(The equations and modifications related information is provided in appendix). Two potentials which we code in CLASS are:

- Exponential potential

$$V(\phi) = V_0 exp(-\frac{\phi}{\phi_a}) \tag{62}$$

- Inverse Square Potential

$$V(\phi) = \frac{n}{4\pi G}\left(1 - \frac{2}{3n}\right)^{\frac{1}{2}} \phi^{-2} \tag{63}$$

We use following data combinations:

- CMB (Planck 2018)
- BAO (Boss Data Release 12, small-z BAO data from 6dF Galaxy Survey and SDSS DR7 main Galaxy sample)
- Combination of the above mentioned CMB and BAO data.
- JLA data.

Exponential Potential

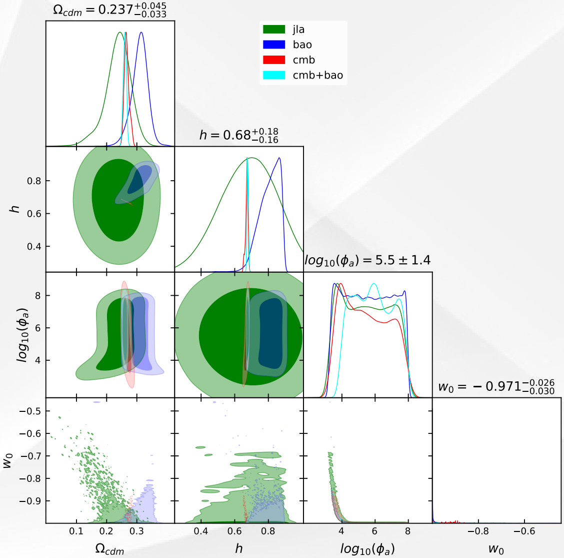

Figure: Triangle plot using four combinations of data, for exponetial potential.

Inverse-Square Potential

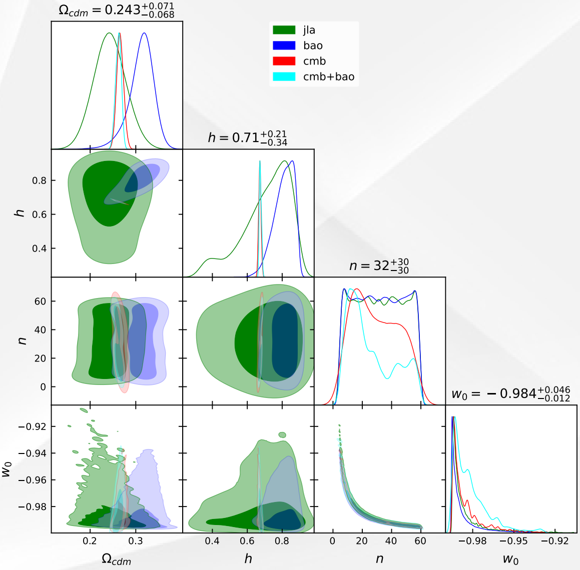

Figure: Triangle plot using four combinations of data, for inverse square potential.

Summary: Linear Perturbations

- We have shown, by recasting equations in a different form, that differences between (linear) perturbations in dependent on the factor of $1 + w$. So for models close to $w = -1$, the differences diminish.
- We validate this by calculating the evolution of potential and its time gradient. For expansion allowed by data, the differences are insignificant.
- Further, we use CMB data to constrain a parametric form of c_s^2 and found that it cannot distinguish between tachyonic and quintessence models.
- Parameters of two common potentials for tachyonic field, exponential and inverse-square potentials, remain weakly constrained by perturbations.

Summary and Prospects

Summary

The main results of these studies are:

- For both, tachyonic fields and quintessence, perturbations in dark energy field are induced by metric perturbations. These grow in time.
- The induced perturbations remain small, even when the matter/metric perturbations have become highly nonlinear.
- Scale of amplitudes is very important for growth of dark energy perturbations. Larger perturbations with small amplitudes evolve to be stronger than those with bigger amplitudes but smaller lengthscales.
- Even though dark energy perturbations are induced and they grow with time, their effect on dark matter or metric is insignificant. This can be attributed to the fact that background is for the most part of expansion history is dominated by dark matter, while dark energy domination is a relatively recent phenomenon.
- Rate of growth of dark energy perturbations is higher(particularly at late times) in nonlinear evolution as compared to linear calculations.
- Effective equation of state (w) becomes a function of spacetime.
- Dynamics of DE perturbations is stronger in large voids and these can be plausible systems for diagnostics of DE perturbations.

Summary...

- We found that the differences in perturbations are dependent on relative differences in background. We simulated perturbations in two models with exactly same background. For backgrounds close to ΛCDM($w \sim -1$), differences are small and increase as we go away from $w = -1$. Dark matter/metric perturbations do not exhibit any significant differences for two different Lagrangians.
- Dark energy fluctuations do show differences, but these differences diminish as background expansion is tuned towards Λ. For background expansion history(or w) constrained by current observations, observables do not show any significant distinguishing features.
- We used linear theory formalism to provide insight into how differences depend on background expansion. Specifically, there is an extra term in equations for quintessence which is proportional to $(1 + w)$.

Summary...

- We used effective speed of sound(of dark energy: c_s^2) formalism to constrain a parametric form of c_s^2 using CMB data(Planck 2018 data release). We found that the parameters are not constrained to distinguish tachyonic models from quintessence.
- We also constrained cosmology for two specific tachyonic models: Inverse-square potential and exponential potential. Parameters of potentials are weakly constrained, while value of Ωs is different from what one would obtained from ΛCDM parameter estimation. This demonstrates the fact the parameter values are dependent on dark energy model assumed.
- **This work suggests that if we are only interested in dark matter perturbations then we may work with any model of dark energy for the given expansion history and may even ignore dark energy perturbations.**

Prospects

- There is a need to explore methods of cosmological simulations, that go beyond linear regime and spherical symmetry in order to study prospects of differentiating between classes of dark energy models. Efforts are needed for simulations that avoid split between background and perturbations. Hence, we would like to explore N-body simulations that are based on relativistic field theory. In the next phase of this research, we plan to study development of numerical/computational methods for such simulations.
- Dynamics of dark energy perturbations in large voids with a focus on identifying observables and degeneracy of these observations with dark matter sector
- A systematic study of linear theory based expansion of Lagrangian, for different types of background expansion, can be done and this can be used for mock predictions for observations from existing/coming experiments.
- The work in this thesis motivates future work on forecast for CMB observations to distinguish different scalar field models.

References

- Manvendra Pratap Rajvanshi and J.S. Bagla,
  Nonlinear spherical perturbations in quintessence models of dark energy,
  Journal of Cosmology and Astroparticle Physics, Volume 2018, June 2018
  doi: 10.1088/1475-7516/2018/06/018 [arXiv:1802.05840]
- Manvendra Pratap Rajvanshi, J. S. Bagla
  Reconstruction of dynamical dark energy potentials: Quintessence, tachyon and interacting models, J Astrophys Astron (2019) 40: 44.
  [arXiv:1905.01103]
- Manvendra Pratap Rajvanshi, J. S. Bagla
  Non-linear spherical collapse in tachyon models and a comparison of collapse in tachyon and quintessence models of dark energy.
  Class. Quantum Grav doi:10.1088/1361-6382/abbb63 [arXiv:2003.07647]
- Manvendra Pratap Rajvanshi, Avinash Singh, H.K. Jassal, and J.S. Bagla,
  Tachyonic vs Quintessence dark energy: linear perturbations and CMB data.[arXiv:2104.00982]